PAPER • OPEN ACCESS

Temperature effect corrections for URAGAN based on CAO, GDAS, NOAA data

View the article online for updates and enhancements.

Temperature effect corrections for URAGAN based on CAO, GDAS, NOAA data

A Dmitrieva[1], N Ampilogov[1], I Astapov[1], N Barbashina[1], V Borog[1], D Chernov[1], A Kovylyaeva[1], R Kokoulin[1], K Kompaniets[1], G Mannocchi[2], Yu Mishutina[1], A Petrukhin[1], O Saavedra[3], V Shutenko[1], O Sit'ko[1], G Trinchero[3], E Yakovleva[1], I Yashin[1]

[1]National Research Nuclear University MEPhI (Moscow Engineering Physics Institute), Moscow, Russia
[2]Istituto di Fisica dello Spazio Interplanetario – INAF, Torino, Italy
[3]Dipartimento di Fisica dell' Universita di Torino et INFN, Torino, Italy

E-mail: ANDmitriyeva@mephi.ru

Abstract. For the analysis of muon flux variations caused by extra-atmospheric processes it is necessary to introduce corrections for meteorological effects. For temperature effect (TE) correction it is necessary to know the temperature profile of the atmosphere. As a rule, this profile is measured by meteorological balloons two or four times a day. Alternative sources are satellite observations and data obtained from models of atmosphere used for weather forecasting. Vertical temperature profiles obtained from NOAA satellites, GDAS (Global Data Assimilation System) and CAO data (Central Aerological Observatory, Russia) for standard isobaric levels were compared. Mean value of temperature difference for most levels does not exceed 1 K. Comparison of URAGAN data corrected for TE with CAO information, satellites and GDAS shows a good agreement. Counting rate and anisotropy of the muon flux corrected for meteorological effects for 2007-2014 are presented.

1. Muon hodoscope URAGAN

URAGAN [1] (Moscow, Russia, 55.7° N, 37.7° E, 173 m a.s.l.) is a wide-aperture precision muon hodoscope (Figure 1) which is used to study atmospheric and heliospheric processes responsible for variations in the muon flux at the Earth surface [2-4]. The hodoscope consists of separate horizontal assemblies (supermodules) with the area of 11.5 m^2 each. Three supermodules of hodoscope (SM) are now under operation in the exposure mode. The supermodule detects muons with high spatial and angular accuracies (1 cm and 1º, respectively) over a wide range of zenith angles (0–80º). Every minute, angular distribution of muons is recorded in a two-dimensional angular matrix $M(\theta,\varphi)$ (θ and φ are zenith and azimuth angles for matrix cell centers, $\Delta\theta = 1º$, $\Delta\varphi = 4º$), which represents a snapshot of the upper hemisphere with 1-minute exposition. One-minute matrix contains ~ 70-80 thousand events.

For the analysis of muon flux variations caused by extra-atmospheric processes it is necessary to introduce corrections for meteorological effects (barometric and temperature) [5].
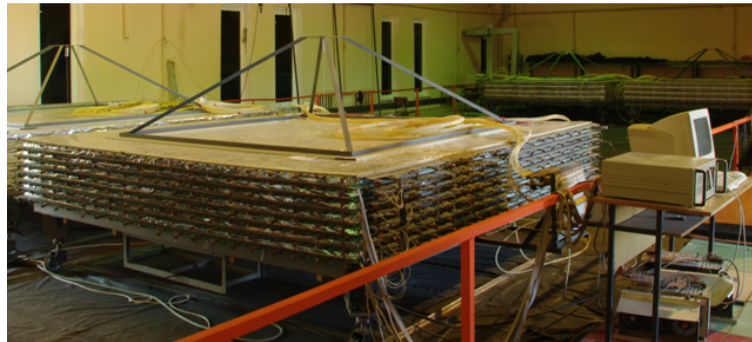
Figure 1. Muon hodoscope URAGAN.

2. Corrections for atmospheric effects

Barometric effect is the anticorrelation of cosmic ray intensity with the pressure at the observation level. Temperature effect is caused by changes of the temperature at all altitudes of the atmosphere. Corrected angular matrix $M^{corr}(\theta,\varphi,t,\Delta t)$ can be calculated by the following way:

$$M^{corr}(\theta,\varphi,t,\Delta t) = M(\theta,\varphi,t,\Delta t) + \Delta M_P(\theta,t,\Delta t) + \Delta M_T(\theta,t,\Delta t), \tag{1}$$

where θ and φ are zenith and azimuth angles for matrix cell centers; $M(\theta,\varphi)$ is the number of reconstructed events in a cell (θ,φ) of the matrix M; t is the time of the beginning and Δt is the time interval of the matrix accumulation; ΔM_T and ΔM_P are corrections for temperature and pressure effects.

$$\Delta M_P(\theta,t,\Delta t) = B(\theta)\cdot(P(t,\Delta t) - P_0), \tag{2}$$

where P is the current pressure at registration level, $P_0 = 993$ mbar is the over a long period averaged pressure at the registration level, $B(\theta)$ are barometric coefficients.

$$\Delta M_T(\theta) = M_0(\theta)\cdot\sum_i W_T(h_i,\theta)\Delta T(h_i)\Delta h_i / 100\%, \tag{3}$$

where $W_T(h,\theta)$ are differential in altitude temperature coefficients (DTC) [6], $M_0(\theta)$ is the over a long period averaged number of reconstructed events for zenith angle θ, $\Delta T(h)=T_{SMA}(h)-T(h)$ is the change of the temperature, h is the atmospheric depth, $\Delta h = 0.05$ atm, $T(h)$ is the current temperature profile of the atmosphere, $T_{SMA}(h)$ is the temperature profile for standard model of the atmosphere [7].

Information about temperature profile of the atmosphere can be obtained from the following sources.

1. Information from direct measurements of air temperature with help of meteorological balloon flights. For example, for URAGAN data correction the information from Central Aerological Observatory (Russia, Dolgoprudny) is used [8,9]. Usually temperature profile is measured by meteorological balloons two times a day: 00:00 and 12:00 UT. Temperature of air is measured at random on altitude points. Unfortunately, sometimes launches of meteorological balloons are not carried out, or balloons do not raise high enough.

2. Another source is the information from meteorological satellites. NOAA-18 and NOAA-19 are weather forecasting satellites run by National Oceanic and Atmospheric Administration (NOAA) [10]. They fly over the Moscow region on average 4 times a day with intervals from 10 minutes to 16 hours. Satellite data about atmosphere can be obtained with the help of the receiving station "Alice-SC", which was installed in MEPhI on the roof of the experimental building of the Scientific and Educational Centre NEVOD in November 2013. Available data of NOAA18 and NOAA19 include:

    – 42 constant pressure levels at which the retrieved values are calculated (in hPa);
    – Date and time of measurement;
    – Latitude and longitude of the current measurement point;
    – Retrieved temperature profile (in K);
    – Temperature guess profile (in K);
    – Water vapor retrieval (in g/kg);

– Dew point temperature retrieval (in K);
– Total-column ozone;
– Cloud fraction;
– Cloud top pressure (in hPa);
– Cloud top temperature (in K);
– Clear/cloud index;
– Effective cloud amount;
– Total precipitable water (in mm);
– Additional data used for retrieval.

3. The alternative sources are weather forecasting models of the atmosphere. One of them is the numerical forecasting model of atmosphere GDAS (The Global Data Assimilation System). GDAS output data are available 4 times a day (at 00, 06, 12, and 18 UTC) for the whole globe (1 degree latitude-longitude grid) and for 23 constant pressure levels (from 1000 to 20 mbar). Retrospective archive data (from 2005 year) are in an open access [11].

3. The comparison of GDAS and NOAA data with CAO data

Vertical profiles of atmosphere temperature obtained from meteorological satellites NOAA and from forecasting model GDAS were compared with direct measurements by meteorological balloons. In the Figure 2, results of two measurements are shown as an example: 23.12.2013 00:00 UTC (on the left) and 22.01.2014 12:00 UTC (on the right). NOAA data is in good agreement with CAO data. But, as one can see, NOAA temperature profile is smoothed and does not reproduce sharp changes in temperature dependence on the pressure level. Comparison of GDAS data with CAO data shows very good agreement.
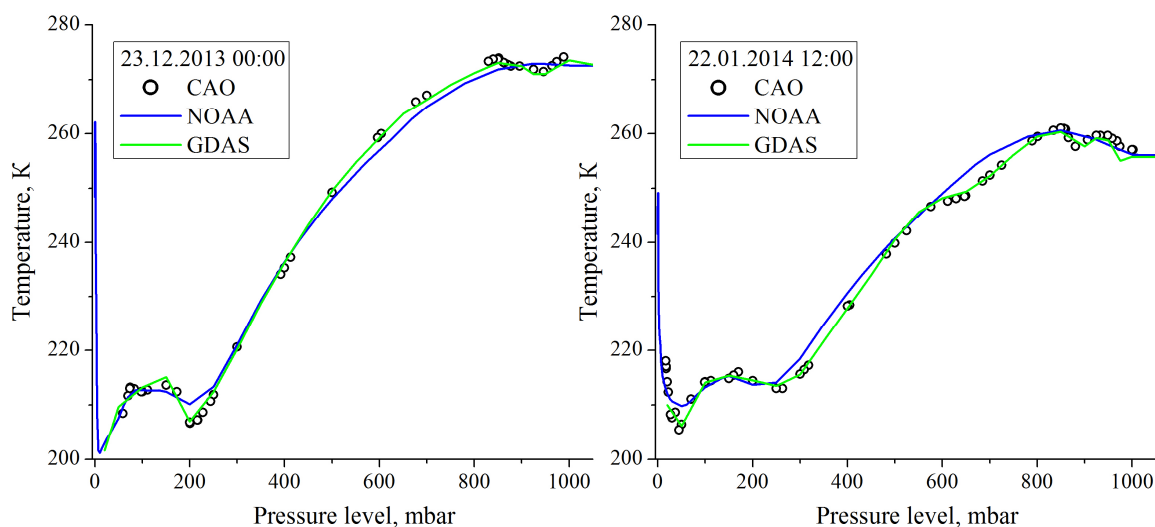

Figure 2. The dependence of air temperature on the pressure level.

Dependence of atmosphere air temperature on time for two pressure levels (50 and 500 mbar) from CAO data and from other sources is shown in the Figure 3. In winter NOAA data is in good agreement with CAO data. But in summer the difference between NOAA and CAO data becomes higher. Comparison of CAO and GDAS data again shows very good agreement.

The dependence of mean value of the temperature difference between data of alternative sources (AS) and CAO ($\Delta T(h,t) = T_{AS}(h,t) - T_{CAO}(h,t)$) on the pressure level is shown in the Figure 4 for NOAA (on the left) and for GDAS (on the right). The shaded region outlines one r.m.s. deviation. For most pressure levels $<\Delta T>$ does not exceed 1 K. So, the temperature profiles of these sources can be used for correction of the muon hodoscope data for the temperature effect.
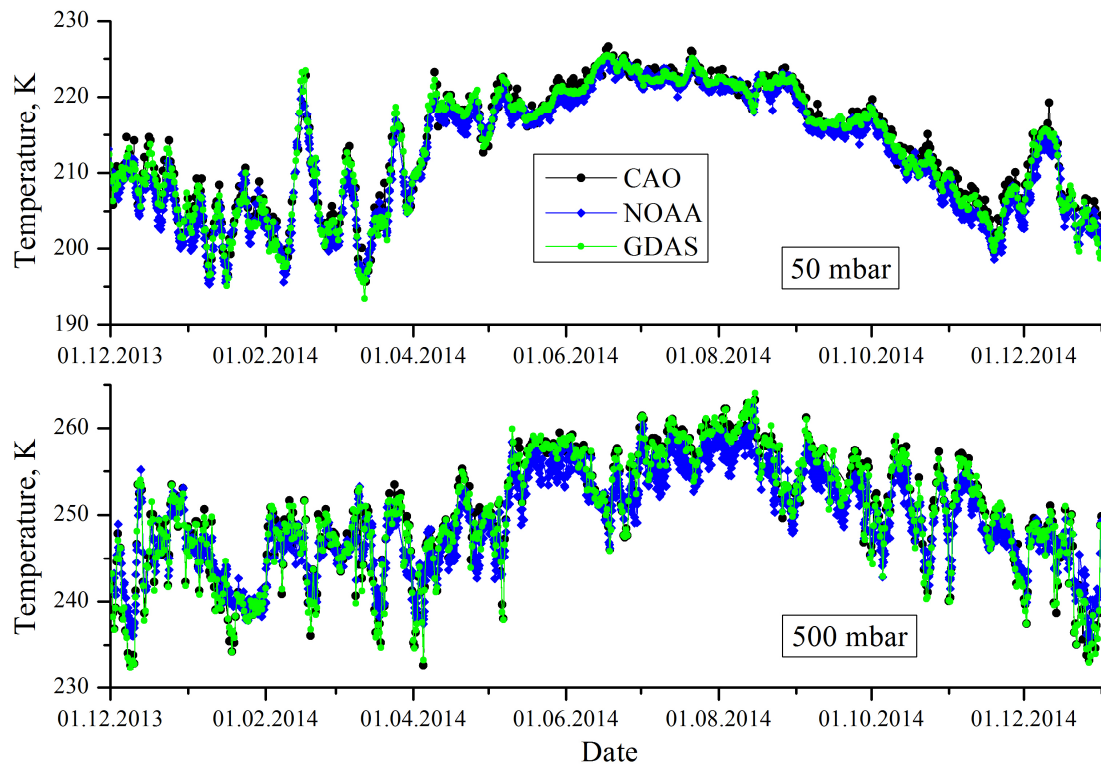
Figure 3. Dependence of atmosphere air temperature on time for two pressure levels.
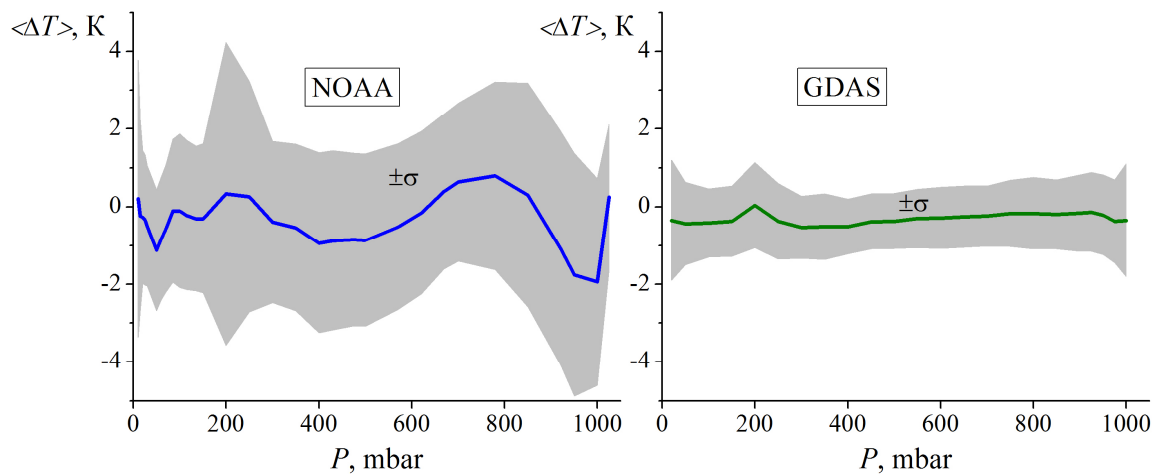

Figure 4. Mean value of temperature difference between NOAA, GDAS and CAO data.

4. Counting rate of the URAGAN hodoscope: 2007-2014

In the Figure 5 (on the top), 1 h average counting rate of the URAGAN hodoscope without and with corrections for meteorological effects is shown. Barometric coefficients for URAGAN slightly depend on zenith angle and are about ~ 0.18%/mbar. After correction for barometric effect, annual variations caused by temperature effect (~ 8 %) become well visible. After correction for temperature effect, variations caused by extra-atmospheric processes appear. For comparison, in the bottom part of Figure 5 the counting rate of Moscow neutron monitor (MNM) corrected for pressure effect [12] is shown. Temperature effect for counting rate of neutron monitors is negligible. URAGAN and MNM are located at the same latitude and have the same threshold rigidity (2.45 GV). But they have different asymptotic directions for primary particles, and besides, muons are sensitive to higher

energies (compared to neutrons) of primary cosmic rays. So, muon hodoscopes open new possibilities for studying the heliospheric perturbations responsible for the modulation at high energies.
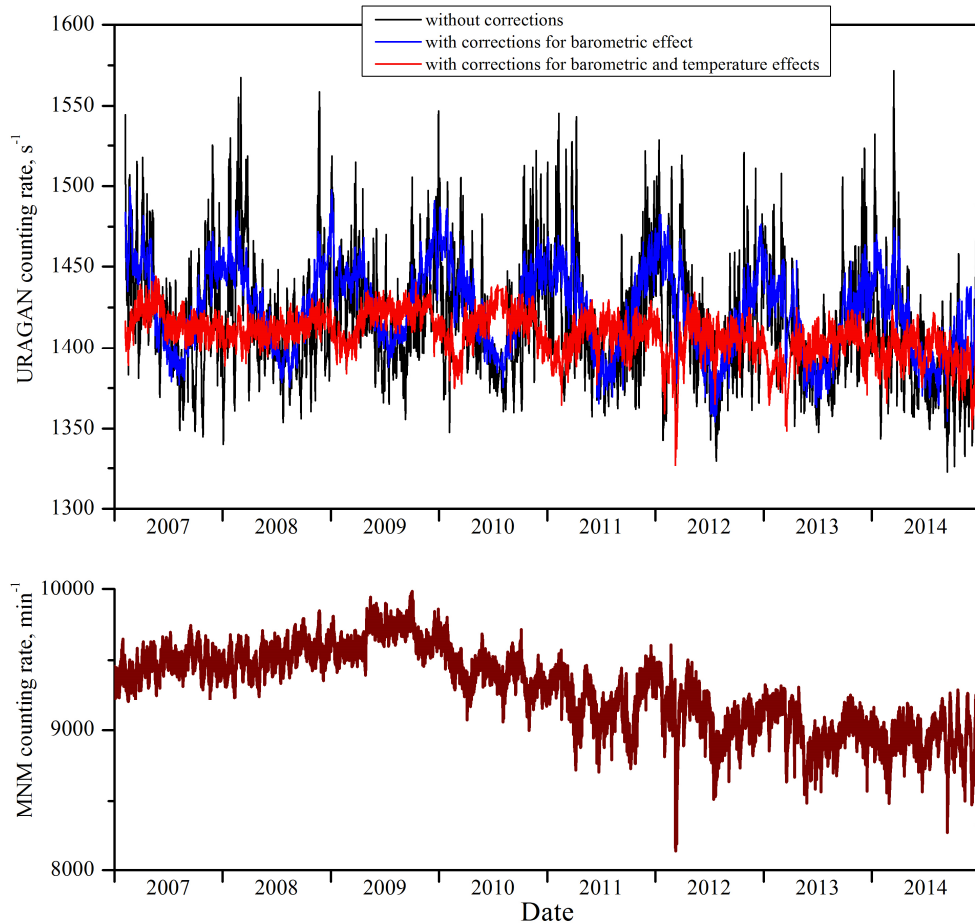

Figure 5. On the top: 1 h average counting rate of the URAGAN hodoscope without and with corrections for meteorological effects. On the bottom: counting rate of Moscow neutron monitor.

URAGAN allows to obtain the vectors of the particle arrival directions and we can use their vector sum. The summary vector normalized to the total number of muons (the vector of local anisotropy) will characterize the angular distribution of the detected particles. The projections of the vector of local anisotropy (A_{South}, A_{East} and A_Z, Figure 6) can be generally defined from the original matrix M data as follows [13]:

$$A_{South} = \frac{1}{N}\sum_{\theta}\sum_{\varphi} M(\theta,\varphi)\cos\varphi\sin\theta \,,$$

$$A_{East} = \frac{1}{N}\sum_{\theta}\sum_{\varphi} M(\theta,\varphi)\sin\varphi\sin\theta \,,$$

$$A_Z = \frac{1}{N}\sum_{\theta}\sum_{\varphi} M(\theta,\varphi)\cos\theta \,,$$

$$N = \sum_{\theta}\sum_{\varphi} M(\theta,\varphi) \,, \qquad A = \sqrt{A_{South}^2 + A_{East}^2 + A_Z^2} \,.$$

(4)

Here N is the total number of events in a given range of angles; A_{South} is the projection on the north–south axis, A_{East} is the projection on the west–east axis; A_Z is the vertical projection. Horizontal projections A_{South} and A_{East} are calculated using the original matrices M without corrections for

barometric and temperature effects. These corrections are annihilated when the values from the opposite azimuthal angles are added, while the use of corrections in the total value (*N*) has almost no effect on the result. The A_Z value was calculated using the values of the matrix without and with corrections for barometric and temperature effects (Figure 7). As one can see, annual variations do not disappear after corrections. According to preliminary estimations, the A_Z projection can be used for the analysis of changes of muon energy spectrum.
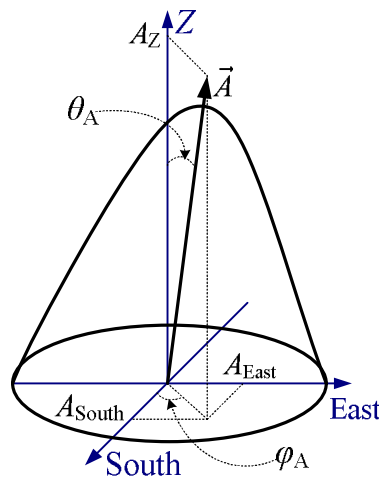

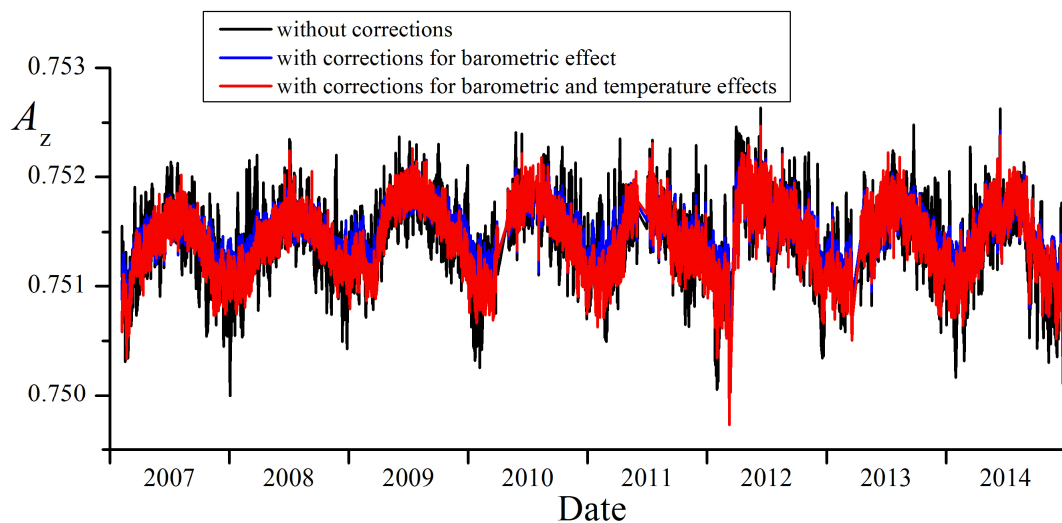Figure 6. The projections of the vector of local anisotropy.

Figure 7. Dependence of vertical projection of the vector of local anisotropy on time.

The comparison of corrections for the temperature effect with the help of satellite data with correction based on data from direct measurements (Figure 8) shows good agreement. So, satellite data can be used for the fast preliminary correction.
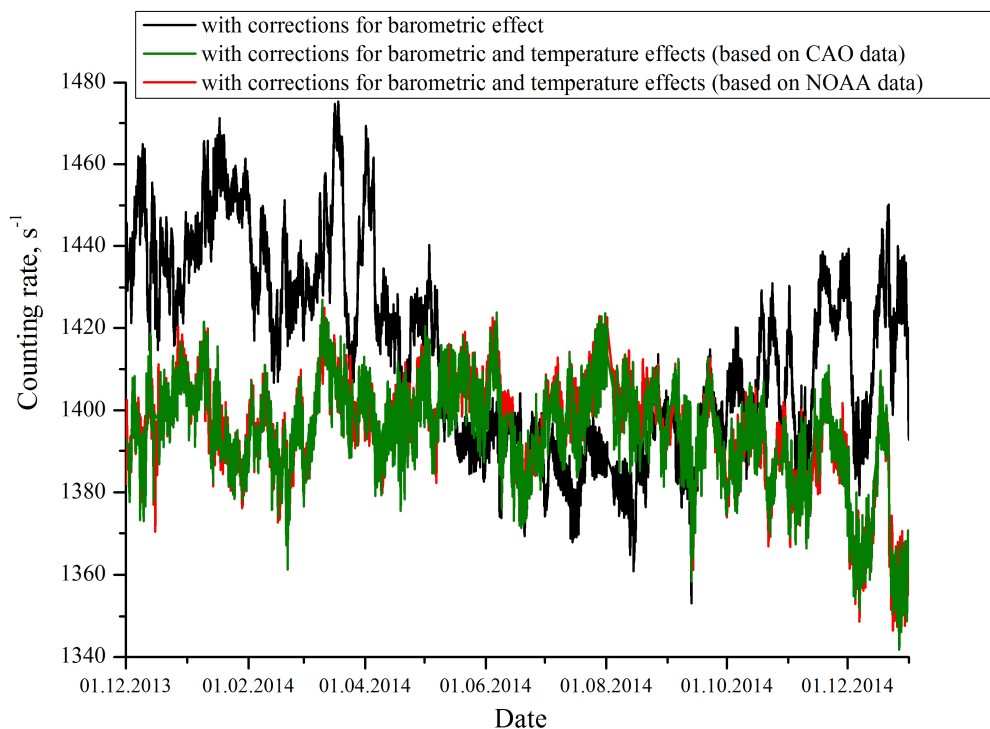
Figure 8. URAGAN counting rate with temperature effect correction based on CAO and NOAA data.

Conclusion

Data of the discussed various sources of the atmosphere temperature profile are sufficiently reliable for the correction of the muon hodoscope counting rate for the temperature effect. Additional retrospective information from CAO and GDAS can be used for temperature effect correction for previous years (since 2005). Satellite data can be used for the preliminary correction in the mode close to real-time (with a delay of only few hours).

Acknowledgments

References

[1]   Barbashina N S *et al* 2008 *Instrum. Experim. Techniques* **51** 180.
[2]   Barbashina N S *et al* 2011 *Bulletin of the Russian Academy of Sciences: Physics* **75** 814.
[3]   Timashkov D A *et al* 2007 *Proc. of the 30th ICRC in Merida, Yucatan, Mexico* **1** 685.
[4]   Ampilogov N V *et al* 2011 *Astrophysics and Space Sciences Transactions* **7** 435.
[5]   Dorman L I 1972 *Meteorological Effects in Cosmic Rays* (in Russian, Moscow: Nauka).
[6]   Dmitrieva A N *et al* 2011 *Astroparticle Physics* **34** 401.
[7]   Glagolev Yu A 1970 *Reference Book on Physical Parameters of the Atmosphere*, Gidrometeoizdat, Leningrad, (in Russian).
[8]   Central Aerological Observatory (Russia, Dolgoprudny): http://www.aerology.org/
[9]   Department of Atmospheric Science of the University of Wyoming: http://weather.uwyo.edu/
[10]   NOAA satellites: http://www.noaa.gov/satellites.html
[11]   NOAA Air Resources Laboratory (ARL), 2004, http://ready.arl.noaa.gov/gdas1.php, Tech. rep.
[12]   Database of Moscow neutron monitor: http://cr0.izmiran.rssi.ru/mosc/main.htm
[13]   Shutenko V V *et al* 2013 *Geomagnetism and Aeronomy* **53** 571.